# A NUMERICAL STUDY OF THE HEAT RECIRCULATION ACROSS THE FLAME-SOLID INTERFACE IN RIM-STABILIZED PROPANE AND N-BUTANE FLAMES

**Leonel Rincón Cancino, M. Eng,** leonel@labcet.ufsc.br
**Amir Antonio Martins Oliveira, Ph.D,** amir@emc.ufsc.br
Combustion and Thermal Systems Engineering Laboratory – LabCET
Dep. of  Mechanical Engineering
Federal University of Santa Catarina
Brazil.

*Abstract. In this work, a numerical study of the flame-solid interaction in propane and n-butane rim-stabilized flames is presented. The fuel-air partially premixed flames (stoichiometric ratio of 0.6) are attached to an orifice in the top side of a circular stainless-steel plate. The flow ranges from laminar to slightly turbulent, which is typical of domestic applications. The analysis employs the κ-ε model for the fluid flow, a global single-step chemical reaction mechanism coupled to the EDC model and allows for conduction heat transfer along the steel plate. The geometry is axisymmetric and the equations are solved using the CFD solver FLUENT. The coupling of the solid and gas phases render the solution expensive in terms of computational time. This is a serious drawback for the use of more complex chemical reaction mechanisms. The results evidence the role of the heat recirculation along the steel plate to the unburned gas mixture in the flame temperature and flame speed. Results are presented for both fuels, evidencing the effects of the ratio between chemical kinetic characteristic time scale and convection-conduction corresponding time scales. Surface heat transfer convection coefficients are also presented.*

*Keywords: Flame-solid interaction, combustion, liquefied petroleum gas, CFD-FLUENT.*

## 1. INTRODUCTION

In many combustion applications, a flame must be ignited by some external means and, after ignition, the reactants need to be continuously mixed and heated by heat transfer from the hot gases, in order to keep the flame burning. This is called flame stabilization. Typically for low power applications, with laminar or slightly turbulent flames, the diffusion or partially premixed flame can be stabilized in the burner rim. In these situations, the metallic surface becomes hot and allows for local ignition (Poinsot and Veynante, 2001; Fernandez et al., 2000). The prediction of the flame stabilization is a complicated matter for numerical combustion codes. When an infinitely fast kinetic model is assumed, it implies that the flame can burn wherever there is fuel and oxidizer, even in those positions where the high heat loss would cause flame quenching. This requires the use of additional assumptions regarding which parts of the flow domain allow for combustion reactions and which parts must be forced to remain inert. Another drawback of these models is that combustion is usually achieved for mass flow rates higher than those that would cause lift off. On the other hand, the use of complex chemical kinetic mechanisms is possible only for simple laminar flame geometries. Specially, when the metallic substrate is included, the strongly different characteristic thermal diffusion length scales requires the use of a large grid refining at the solid-gas interface in order to capture reaction and boundary layer effects.

Here, a flame stabilized in an orifice in a circular plate is modeled. In this situation, the flame exchanges heat to the topside of the plate. Heat conduction along the plate and surface convection then preheats the incoming reactant mixture in the bottom side. Figure 1 presents a rendering of the coupled heat transfer in the gas and solid phases.
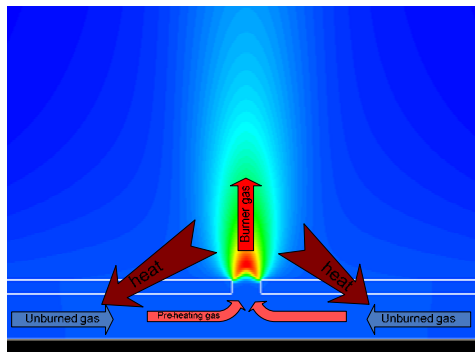


**Figure 1**: Rendering of the heat recirculation from burned to unburned gas mixture.

The main objective here is to estimate the effect of the heat recirculation across the plate in the final flame temperature and configuration. Although a complete calculation for a rim-stabilized flame is extremely complicated, some estimates of the heat exchanged between the flame and the surface can be made using RANS models. Care must be take in properly accounting for some chemical kinetic limitation and this has been done using the Eddy-Dissipation Concept model connected to a single-step chemical reaction mechanism, following the procedure available in FLUENT.

In the following, the geometry and model adopted are presented and the main findings, along with their limitations, are discussed.

## 2. MODELING AND SIMULATION

### 2.1 Description of the problem and geometry

In this work, a flame is stabilized on an orifice injector on top of a circular steel plate. The reactant mixture flows in a channel formed by the space under the plate. The mixture with an initial fuel-rich composition flows steadily under the plate and is injected in a quiescent infinite ambient. The ambient air provides the additional oxygen to complete the combustion reactions. Therefore, the flame has a partially premixed character. The primary reactant mixture mass flow rate is chosen such as to create slightly turbulent flames. An axissymetric geometry is employed in order to minimize computational requirements. The thickness of the plate is e = 0.6 mm, the diameter of the injection hole is d = 1.3 mm and the channel size (under the plate) is b = 2 mm. Figure 2 shows the main dimensions of the computational domain. In order to avoid far-field effects values of D = 70 mm and H = 90 mm were adopted.

### 2.2 Combustion model

In a combustion process, several thousands of chemical reactions occur simultaneously (Cancino 2004, Cancino and Oliveira 2004, 2005, 2005b) and several hundreds of chemical species are involved. For the methane – air reacting system, the GRIMech 3.0 reaction mechanism includes 354 chemical reaction and 53 chemical species. For heavier hydrocarbons the situation becomes even more complicated. A detailed kinetic model for the iso-octane oxidation can be composed by a set of about 4000 chemical reactions (Curran, 2002). CFD programs applied to combustion need to resolve the full set of conservation equations for mass, linear momentum, energy (including radiation), turbulence variables and one additional equation for the conservation of the mass for each chemical species considered in the combustion process, besides the ideal gas law and equations for the thermodynamic properties. When the flow is turbulent, the equations have to be solved in the full transient form. This method of solution named DNS (Direct Numerical Simulation) is a formidable task even for solvers that employ the state-of-the-art in computational methods in heavily parallelized machines (Westbrook, 2005) and is basically employed to very idealized situations. The alternative to a full solution of the flow and combustion is modeling. The next two basic levels of modeling are the use of LES (Large Eddy Simulations), in which the larger eddies are resolved in a full transient simulation while the effect of the smaller turbulent eddies is modeled, and RANS (Reynolds-Averaged Navier-Stokes) models, in which the equations are time averaged and the interaction between the turbulence and the chemical kinetics is approximately accounted for. RANS models are widely used because of smaller computational requirements. The drawback is the lesser accuracy of the results obtained, which can, eventually, lead to wrong conclusions. Care must be exercised not to exceed the predictive nature of these models.

In RANS models, the time-averaged chemical reaction rates are estimated using one of three treatments (Stefanidis, 2006): a) statistical approaches, b) flamelet models, and c) models relating the chemical reaction rates to functions of time-averaged properties. In the first group are the Provability Density Function PDF models. In the second group are the models based in a geometrical analysis of the flame; considering the reactions to be sufficiently fast so that the length scale of the reaction zone is smaller than the Kolmogorov length scale. In this case, the flame can be considered as an ensemble of very thin, isotropic, one-dimensional laminar flame structures (flamelets). In the third group are the models that relate the time-averaged reaction rates to turbulent mixing levels and this is the model used here.

Here, the standard $\kappa$ - $\varepsilon$ model for turbulence is used. This model is based on solution of conservation equations for the Turbulent Kinetic Energy ($\kappa$) and the Dissipation Rate of Turbulent Kinetic Energy ($\varepsilon$). A global kinetics with a one-step reaction models the combustion chemistry. The coupling to turbulence is done using the Eddy-Dissipation Concept EDC model (Magnussen and Hjertager, 1976; Magnussen, 1981, 1989). In this model, we assume that there is complete molecular mixing of reactants and products within the smallest turbulent scales, with dimensions proportional to the turbulent kinetic energy dissipation characteristic length scales (Kolmogorov scales). Within these small regions, called the inner region, there is a chemical reaction, controlled by a chemical reaction mechanism, transforming reactants to products. Here, the global one-step mechanism presented in Eq. 1 is used. Between the inner region and the outer region, there is reactants and products turbulent transport, controlled by the larger scales turbulent transport mechanisms. The local mass balance requires that the net mass flux of each chemical species $i$ between both regions (in and out) is equal to the inner region chemical reaction rate.

In this model, the volumetric fraction of the flow occupied by turbulent smaller scales (inner region) is given by $\xi^3$ where $\xi$ is defined by:

$$\xi = C_\xi \left(\frac{\nu \varepsilon}{k^2}\right)^{1/4} \tag{1}$$

where $C_\xi$ is a volumetric fraction constant equal to 2.1377 and $\nu$ is the kinematic viscosity.

Mass renewal inside the small scales region occurs in a characteristic time given by:

$$\tau = C_\tau \left(\frac{\nu}{\varepsilon}\right)^{1/2} \tag{2}$$

where $C_\tau$ is a time scale constant equal to 0.4082.

The net mass flux between the inner and outer regions is given by:

$$R_i = \frac{\rho \xi^2}{\tau(1-\xi^3)}\left(Y_i^* - Y_i\right) \tag{3}$$

where $Y_i^*$ is the mass fraction of chemical species $i$ existing in the inner region. This model assumes one for the probability of reaction, denoted by $\chi$ in Magnussen original work (Magnussen, 1981, 1989).

The inner region mass balance requires that the net mass flux be proportional to the molecular chemical reaction rate, which means

$$R_i^* = \frac{R_i}{\xi^3} \tag{4}$$

From the equation for the net mass flux, the mass and energy balances result in:

$$\frac{\rho^*}{\tau(1-\xi^3)}\left(Y_i^* - Y_i\right) = R_i^* \qquad ; \qquad \frac{\rho^*}{\tau(1-\xi^3)}\left(h^* - h\right) = q^* \tag{5}$$

where $\rho^*$ is the mixture specific mass of small scales region and $h^*$ and $h$ are the mixture enthalpies of small scales and mean flow regions given by:

$$h^* = \sum_1^N Y_i^* h_i^* \quad ; \qquad\qquad h = \sum_1^N Y_i h_i \tag{6}$$

where $N$ is the number of chemical species present in the mixture.

For the chemical reaction rate, the inner region can be modeled as a Perfectly Stirred Reactor (PSR). For a global mechanism reaction rate, we assume an Arrhenius model, given by:

$$R_i^* = \frac{M_i}{n_i}\left[AT^\beta \exp(-E/RT)\right] X_{CH_4} X_{O_2}^2 \tag{7}$$

where $A$ is the pre-exponential factor, $E$ is the activation energy, $\beta$ is a temperature coefficient, $R$ is the universal constant of gas, $M_i$ is the molecular mass of chemical species $i$ and $n_i$ is the stoichiometric coefficient of chemical species $i$ in Eq. (1).

The gas mixture is assumed to follow an ideal gas behavior, then,

$$p = \rho T R \sum_{i=1}^N \frac{Y_i}{M_i} \quad ; \qquad h_i = h_{i,f}^o + \int_{T_o}^T c_{p,i} dT \quad ; \qquad h_i^* = h_{i,f}^o + \int_{T_o}^{T^*} c_{p,i} dT \tag{8}$$

where $c_{p,i}$ is the specific heat of chemical species $i$ and $h_{i,f}^o$ is the standard enthalpy of formation.

The system of equations valid in the small scales is solved for each control volume, in the form of a sub-grid model. From this solution, temperatures $T^*$ and concentrations $Y_i^*$ in the small scales region are obtained. This data, with local mass fraction $Y_i$, is then used to obtain the local average volumetric reaction rate from Eq. (3).

For the sake of comparison to the results obtained from the EDC model, results are also obtained with the standard Eddy Break Up (EBU) model, which is equivalent of assuming extremely fast reaction rate kinetics.

Gas radiation has been neglected.

## 2.3 Simulation model

A 2D axial-symmetric geometry is used, in order to reduce the computational effort. A hybrid structured/unstructured mesh is used, with the care of deploying a refined grid along the solid-gas interface. Figure 2 presents a view of the mesh generated.
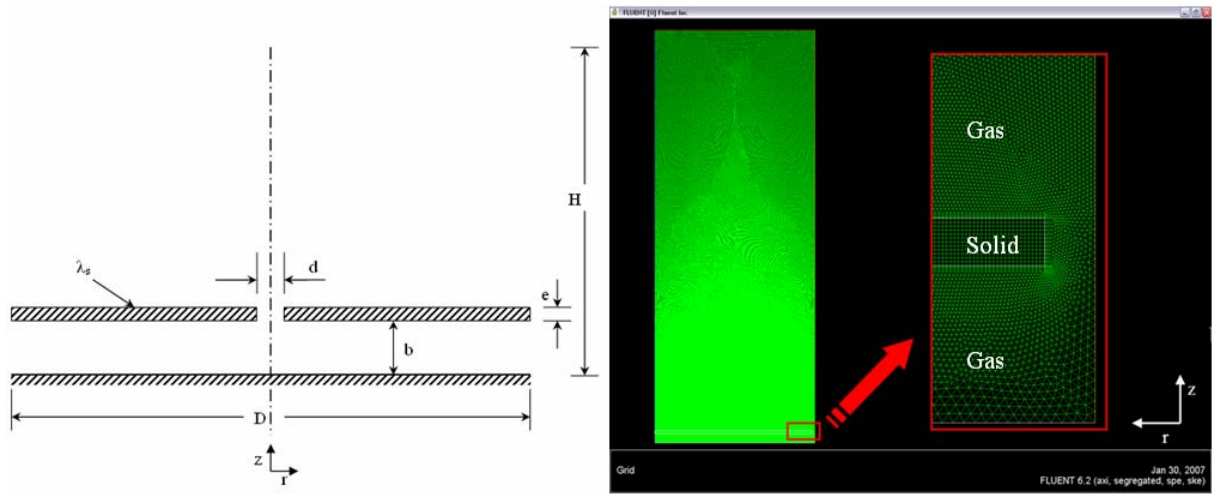


**Figure 2**: Geometry and computational mesh.

The fluid and solid phases are thermally coupled; which allows the heat recirculation in the two phases. The solution is set up such that reaction is only allowed in the upper gas domain above the upper surface of the plate (and hole). A full multicomponent diffusion model is used. A grid study was performed and a mesh with about 300,000 points was found adequate for the solution. Two fuels are considered in this work, butane ($C_4H_{10}$) and propane ($C_3H_8$), and the temperature dependent properties are obtained from the program's library. Table 1 presents the computational cases that were solved. The primary air stoichiometric ratio was fixed in 0.6 (fuel-rich). The ractant mixture is admitted to the computational domain at 300°C.

**Table 1**: Cases considered in this work for simulation.

| | Fuel | Oxidant | Stoichiometry | b (mm) | e (mm) | d (mm) | D (mm) | H (mm) | Turbulence model | Turbulence-chemical kinetics interaction model |
|---|---|---|---|---|---|---|---|---|---|---|
| **case 1** | Propane | Air | 0.6 | 2 | 0.6 | 1.3 | 70 | 90 | k-e | ED |
| **case 2** | Propane | Air | 0.6 | 2 | 0.6 | 1.3 | 70 | 90 | k-e | EDC |
| **case 3** | Butane | Air | 0.6 | 2 | 0.6 | 1.3 | 70 | 90 | k-e | ED |
| **case 4** | Butane | Air | 0.6 | 2 | 0.6 | 1.3 | 70 | 90 | k-e | EDC |
| Inlet Temperature of the reactants and Room Temperature = 300 K ||||||||||| |

## 3. RESULTS AND ANALYSIS

The results presented are the solid wall temperature and heat transfer rate and the gas velocity and temperature field.

### 3.1 Analysis fo the gas phase

Figure 3 presents the temperature field and Figure 4 presents the velocity field for butane modeled with EBU and EDC. From the temperature fields in Figure 3, it can be noticed that the EBU model results in a hotter flame attached more closely to the orifice. From Figure 4, it can be seen that the EBU model predicts larger velocities than the EDC

model. The EBU model calculates fluid velocities at the flame front of the order of 3.0 m/s for a Reynolds number, based on the orifice diameter, of approximately 2.5. This results in a longer flame than that obtained for the EDC model. The EDC model, on the other hand, results in fluid velocities at the flame front of the order of 0.8 m/s, with essentially the same orifice Reynolds number of 2.5. The values of velocity obtained with the EBU model are more reasonable. The same trends are calculated for propane. This shows that chemical kinetics is controlling the time-averaged reaction rates in the EDC model.

Figure 5 presents the distribution of turbulent kinetic energy. It can be observed a production of kinetic energy along the edges of the orifice and along the flame front. The EBU model results in larger production of kinetic energy, which results in a fictitious larger value of time-averaged reaction rate, stabilizing the flame closer to the orifice. The EDC model, in the other hand, results in a flame stabilized higher above the orifice.
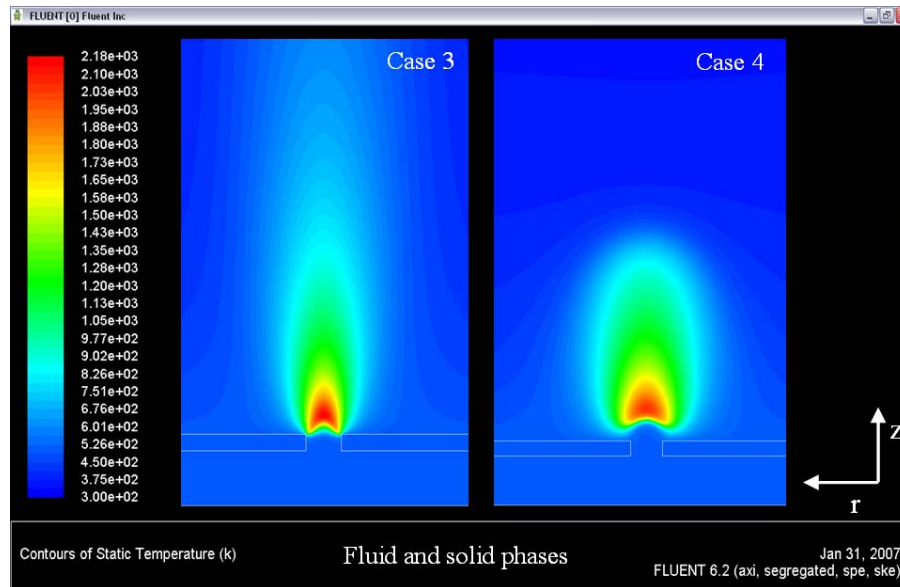


**Figure 3**: Temperature distributions in the solid and fluid phases.
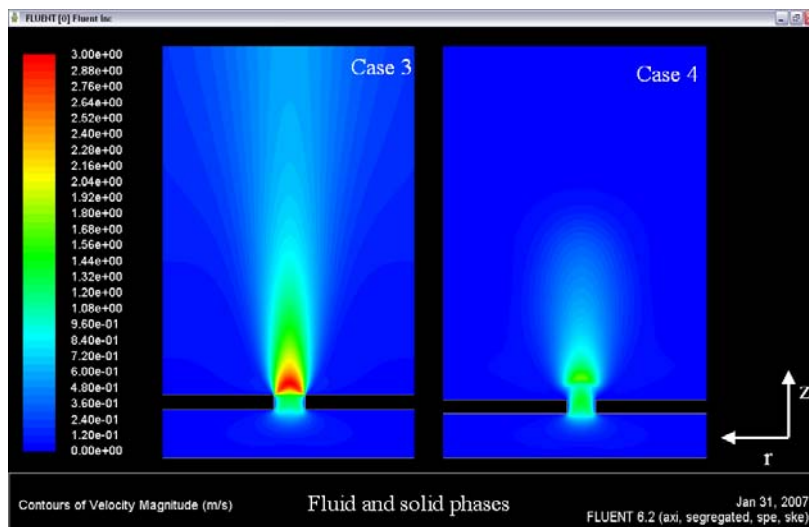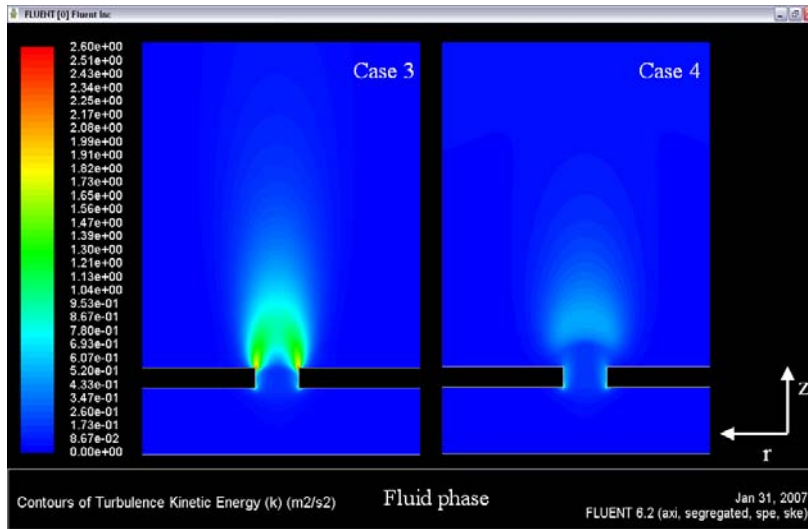


**Figure 4**: Velocity fields in the gas phase for butane using (3) EBU and (4) EDC.

**Figure 5**: Contours of turbulent kinetic energy for butane using (3) EBU and (4) EDC.

Figure 6 presents axial temperature and velocity distributions in the first few millimeters of an axis that follows the orifice centerline (z axis). The inner channel thickness is 2 mm and the plate thickness is 0.6 mm. It can be seen the larger temperature and velocity that result from the EBU when compared to the EDC model. As a result, the flame is anchored closer to the orifice in the EBU model. The velocity calculated for the EDC model shows an initial increase as a result of the expansion suffered by the reactant gas phase when it is preheated by the plate close to the orifice, followed by a decrease, caused by the area expansion as soon as it leaves the orifice, and finally, followed by another increase as the gas phase crosses the flame region. The velocity profile calculated from the EBU model does not show the local maximum because the flame is closer to the plate, overlapping the plate preheating to the flame preheating.
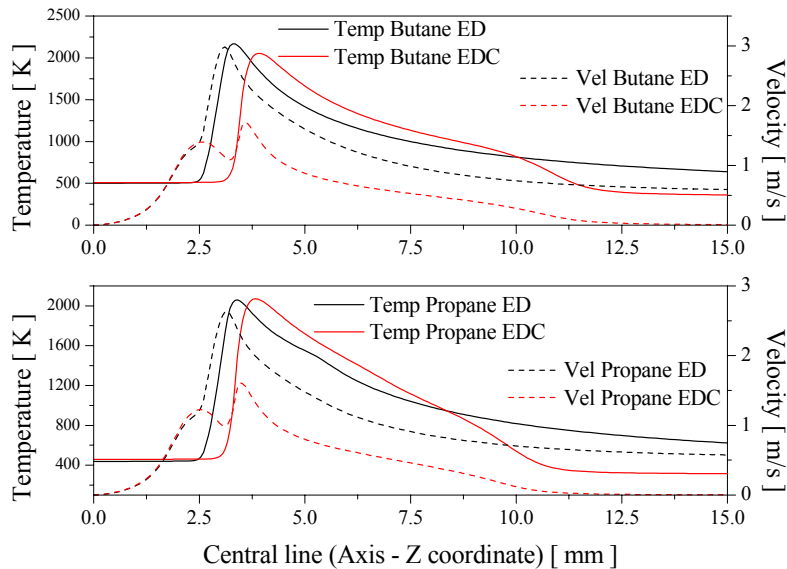


**Figure 6**: Temperature and velocity distribution in the central line of the computational domain.
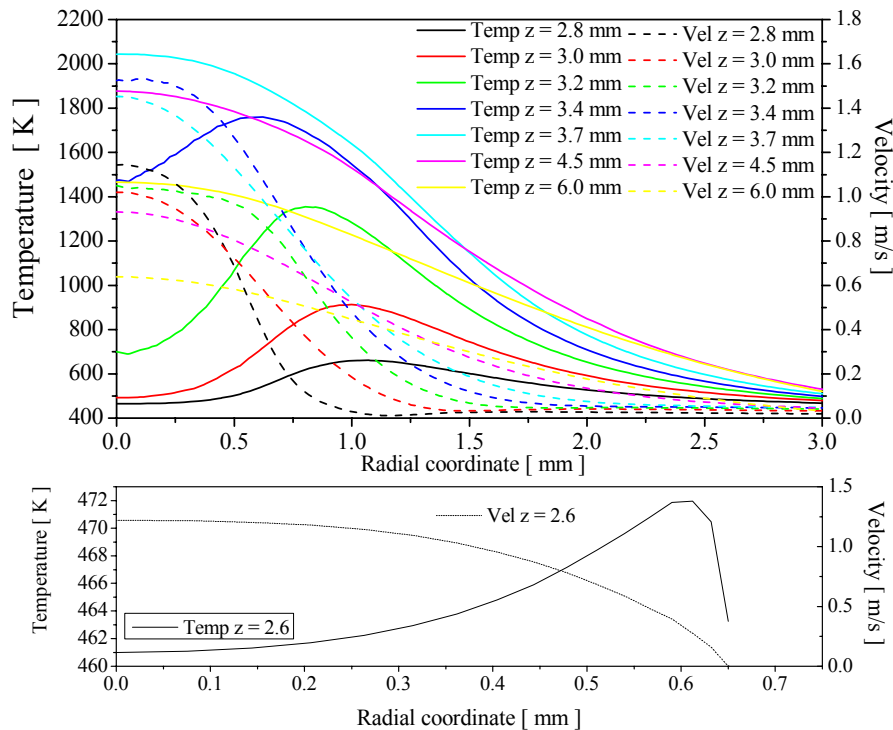
**Figure 7**: Temperature and velocity profiles, case 2, Propane-air with EDC model.

Figure 7 presents radial distributions of temperature and velocity for butane and propane for different axial distances. The first radial profile corresponds to the orifice outlet at z = 2.6 mm. We note that the temperature has a maximum near the plate wall as a result of the preheating. The reactants are admited to the computational domain at 300°C and right at the orifice exit the temperature near the plate reaches 461°C. The velocity has an approximately parabolic profile. As distance z increases the temperature peak increases and moves to the centerline. Once the flame front is crossed, the temperature decreases again. Velocity has a similar trend, but decreases before the maximum temperature is reached.

### 3.2 Analysis of the solid phase

Figure 8 presents the radial and axial temperature distribution in the solid phase (plate) for the four cases simulated, whose conditions are described in Table 1. Combustion takes place in the upper-left side of the plate. The plate temperature is larger for butane than for propane. The low heating value for propane is 46,357 kJ/kg while the low heating value for butane is 45,742 kJ/kg (Turns, 2000).

Figure 9 presents the surface temperature in the internal and external walls of the plate for the four cases. We can observe that after the first 2 mm of length the internal and external temperatures of the plate reach the same value, due to lateral conduction heat transfer. This indicates that the majority of the heat transfer from the burned gases to the reactant mixture occurs in the first millimeters in the radial direction.

Figure 10 presents the surface heat transfer profile along the upper and bottom plate surfaces. Along the external wall, the heat transfer rate changes sign over the plate at a distance of about 4 mm from the centerline. In the first 4 mm the heat transfer flux goes from the gas to the solid phase and after 4 mm, it goes from the solid to the gas phase. In the bottom wall, however, the heat flux is always from the solid to the gas phase, preheating the reactants. From the local surface temperature and normal gas temperature profile, the local surface convection coefficient can be estimated. For the EDC model, values of 142 W/m²-K and 82 W/m²-K were obtained for butane and propane at the orifice edge.

Figure 11 presents a rendering summarizing the trends in the heat transfer from the gases to the plate.
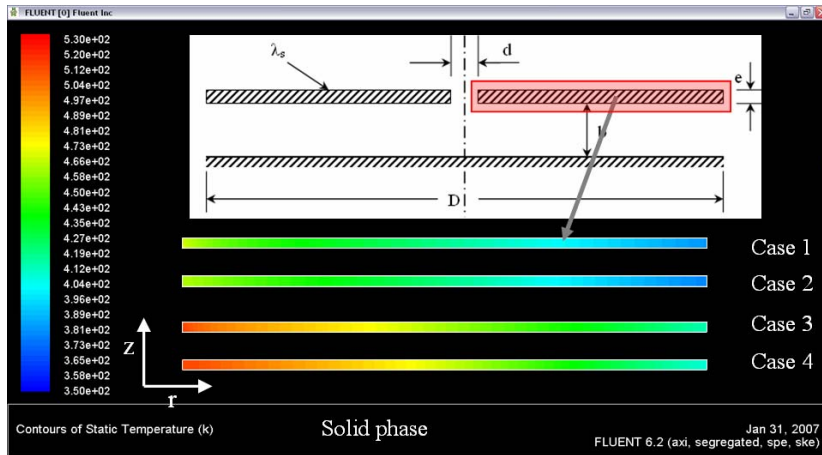
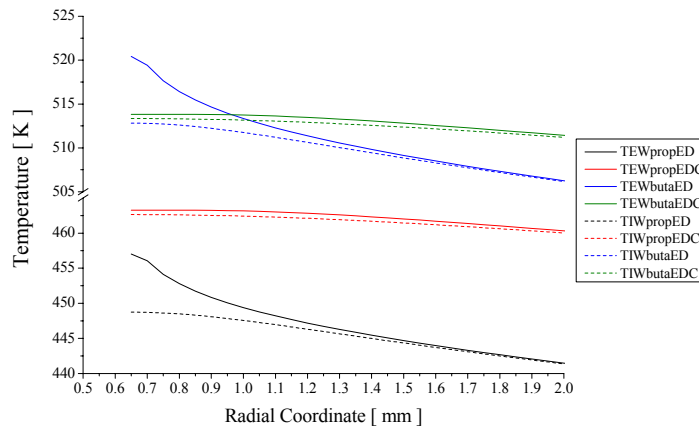**Figure 8**: Temperature distributions in the solid phase (plate).



**Figure 9**: Surface temperature distributions in the internal and external walls of the plate.
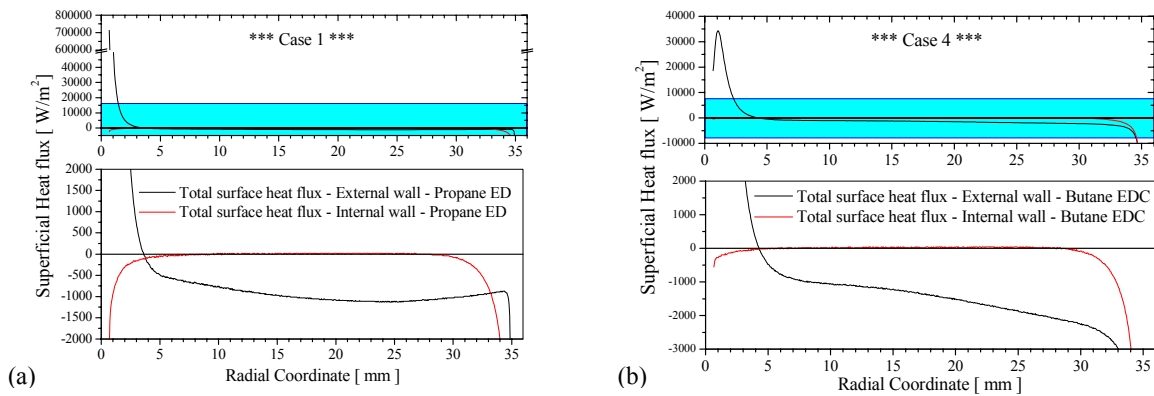


**Figure 10**: Total surface heat flux in the external and internal walls of the plate (solid domain).
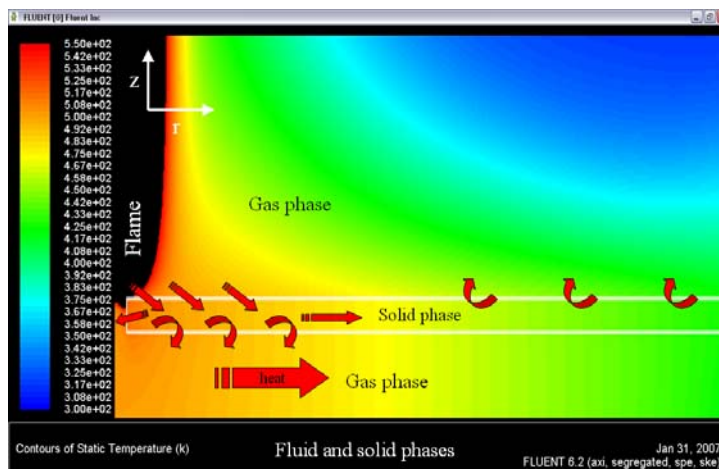
**Figure 11**: Heat recirculation pattern in the solid and fluid phases.

## 4. CONCLUSIONS

Here, a numerical study of the flame-solid interaction in propane and n-butane rim-stabilzed flames is presented. The analysis employs a turbulence model (κ-ε model) and a global single-step chemical reaction mechanism for the gas phase and conduction heat transfer along the orifice plate. The coupling of the solid and gas phases render the solution expensive in terms of computational time. This is a serious drawback for the use of more complex chemical reaction mechanisms. The computational time for each simulation was 25 days using two Pentium IV, 3.4 GHz, in parallel processing and 4 GB of RAM (Random Access Memory) memory. The difference in the computational time between the EBU and EDC models is small. However, the EDC model presents a higher convergence difficulty in the beginning of the computation (firsts 10 days…) when it is imposed one iteration of the chemistry for each iteration of the fluid-dynamic equations. The results evidence the role of the heat recirculation along the steel plate to the unburned gas mixture in the flame temperature and flame speed.

## 5. ACKNOWLEDGEMENTS

## 6. REFERENCES

Cancino, L. R., 2004, "Análise de equilíbrio químico, cinética química da ignição térmica e propagação de chama plana laminar de misturas de hidrocarbonetos leves com ar". Dissertation of Master degree at the Federal University of Santa Catarina, 2004, in Portuguese, 245 pp.

Cancino, L. R. and Oliveira, A. A. M., 2005 b, "Analysis of the thermal ignition and induction time of premixed ethanol and air combustion". Proceedings of the 18th International Congress of Mechanical Engineering. COBEM 2005. Brazil.

Cancino, L. R. and Oliveira, A. A. M., 2004, "Análise de equilibrio químico, cinética química da ignição térmica e propagação de chama plana laminar de misturas de hidrocarbonetos leves com ar". Proceedings of the ENCIT 2004, Rio de Janeiro, Oct. 2004, 11 pp.

Curran, H. J., Gaffuri, P., Pitz, W. J. and Westbrook, C. K., "A Comprehensive Modeling Study of iso-Octane Oxidation", Lawrence Livermore National Laboratory, Livermore, CA 94551, USA, 2002,

Fernandez, E., Kurdyumov, V. And Linan, A., 2000, Diffusion flame attachement and lift-off in the near wake of a fuel injector, 28th Symposium (Int.) on Combustion, The Combustion Institute, Pittsburg.

Fluent 6.2 Documentation. Fluent Inc.

GRIMech Gas Research Institute. Disponível em: < http://www.me.berkeley.edu/gri_mech/ > GRIMech 3.0 (2000).

Heynderickx, G.J., Stefanidis, G.D., Merci, B., Marin, G.B. "CFD simulations of steam cracking furnaces using detailed combustion mechanisms" Computers and Chemical Engineering 30 (2006) 635–649.

Poinsot, T. and Veynante, D., 2000, Theoretical and Numerical Combustion, Edwards, Philadelphia, EUA.

Stefanidis, G.D., Merci, B., Heynderickx, G.J., Marin G.B. "CFD simulations of steam cracking furnaces using detailed combustion mechanisms", Computers and Chemical Engineering 30 (2006) 635–649.

Westbrook, C, K., Mizobuchi, Y., Poinsot, T, J., Smith, S., Warnatz, J. "Computational Combustion." Proceedings of the Combustion Institute. 30 (2005). 125-157.

Wilcox, D. C. "Turbulence modeling for CFD" DCW Industries, INC. La Cañada, California. 1994.

**7. RESPONSIBILITY NOTICE**

The author(s) is (are) the only responsible for the printed material included in this paper.